Magn Reson Mater Phy (2011) 24:225–232
DOI 10.1007/s10334-011-0256-9

RESEARCH ARTICLE

Assessment of neovascular permeability in a pancreatic tumor model using dynamic contrast-enhanced (DCE) MRI with contrast agents of different molecular weights

Louke J. Delrue · Veerle Casneuf · Nancy Van Damme · Peter Blanckaert · Marc Peeters · Wim P. Ceelen · Philippe C. O. Duyck

Received: 18 November 2010 / Revised: 6 April 2011 / Accepted: 26 April 2011 / Published online: 13 May 2011

Abstract
Object We evaluated the relationship of dynamic contrast-enhanced magnetic resonance imaging (DCE-MRI)-derived pharmacokinetic parameters and contrast agents with different molecular weights (MW) in a pancreatic tumor mouse model.
Materials and methods Panc02 tumors were induced in mice at the hind leg. DCE-MRI was performed using Gadolinium (Gd)-based contrast agents with different MW: Gd-DOTA (0.5 kDa), P846 (3.5 kDa), and P792 (6.47 kDa). Quantitative vascular parameters (AUC, K^{trans}, V_e, and V_p) were calculated according to a modified Tofts two-compartment model. Values for all contrast groups were compared for tumor and control (muscle) tissues.
Results Values for K^{trans} and V_e were significantly higher in tumor tissue than in muscle tissue. When comparing contrast agents, lowest absolute K^{trans} values were observed using P792. The relative increase in K^{trans} in tumor tissue compared with normal tissue was highest after the use of P792. In both tumor and normal tissues, K^{trans} decreased with increasing molecular weight of the contrast agent used.
Conclusion It was demonstrated that values for the different DCE-MRI vascular (permeability) parameters are highly dependent on the contrast agent used. Due to their potential to better differentiate tumor from muscle tissue, higher molecular weight contrast agents show promise when evaluating tumors using DCE-MRI.

Keywords DCE-MRI · MRI contrast · Gd-DOTA · P792 · P846

L. J. Delrue (✉) · P. Blanckaert · P. C. O. Duyck
Department of Radiology, Ghent University Hospital, De Pintelaan 185, 9000 Gent, Belgium
e-mail: Louke.Delrue@uzgent.be

P. Blanckaert
e-mail: peter.blanckaert@ugent.be

V. Casneuf · N. Van Damme · M. Peeters
Department of Gastro-Enterology, Ghent University Hospital, De Pintelaan 185, 9000 Gent, Belgium

W. P. Ceelen
Department of Gastrointestinal Surgery, Ghent University Hospital, De Pintelaan 185, 9000 Gent, Belgium

Introduction

Pancreatic cancer (PC) accounts for more than 35,000 deaths in the United States annually (36,800 estimated deaths in 2010). Five-year survival rate from 1999 until 2005 was about 6% [1]. Development, growth, and metastasis of malignant pancreatic tumors are regulated by angiogenesis, the generation of new blood vessels from preexisting vasculature [2–4]. The newly grown capillary vessels differ from normal capillaries. Several studies have demonstrated that vessels of malignant tumors have an increased permeability caused by morphologic endothelial changes [5–7]. As the process of neo-angiogenesis plays an important role in the growth and spread of tumors, it is also recognized as a significant independent predictor of overall survival rate [8]. Measurement of angiogenesis can serve as a prognostic marker in oncology.

Dynamic contrast-enhanced magnetic resonance imaging (DCE-MRI) combined with pharmacokinetic modeling is a promising noninvasive imaging technique for the in vivo characterization of tumor angiogenesis and for the in vivo evaluation of therapy-induced microvascular changes [7,9–12]. We have previously shown that $T1$-weighted DCE-MRI using a macromolecular contrast agent (CA) allows quantification of several kinetic parameters that relate to tumor physiology [13,14].

The main parameter of interest is neovascular permeability, which is known to be a sensitive surrogate marker of tumor angiogenesis [15]. The relevant kinetic parameter is the (endothelial or volume) transfer constant or K^{trans}. Clinical studies in a variety of cancer types have demonstrated that DCE-MRI with kinetic modeling allows to differentiate benign from malignant tumors and, importantly, to provide a tool for early therapy response imaging and quantification [16–22]. The physiological significance of the calculated K^{trans} depends on a number of variables, the most important of which are the size and physicochemical properties of the CA used. Indeed, when using a small, highly diffusible CA, the measured K^{trans} will mainly reflect tissue perfusion rather than microvascular permeability. The choice of the CA is therefore to be adapted to the specific tumor model and physiological property under scrutiny.

This study was designed to evaluate DCE-MRI-based kinetic modeling using contrast agents with different molecular weights in a mouse model of pancreatic cancer.

Materials and methods

Animal model

Male HsdOla/MF1 mice ($n = 30$, 4–6 weeks old, 16–20 g body weight) were obtained from Harlan Laboratories (the Netherlands) and housed in standard facilities at the Department of Laboratory Medicine, Ghent University, Belgium. All procedures were in compliance with the guidelines and regulations for use, maintenance, and care of animals and approved by our institutional committee for animal care, Faculty of Medicine, Ghent University, Belgium.

Panc 02 cells (Panc 02 is a murine ductal pancreas carcinoma cell line, established in 1984 in female C57B1/6 mice; Panc 02 cells were provided by the Department of Surgery, University of Heidelberg, Germany) were cultured in RPMI1640 medium (Invitrogen Corporation, Gibco, Merelbeke, Belgium) supplemented with 10% fetal calf serum (Invitrogen Corporation), 4 mM L-glutamine, 50 μL/ml penicillin, and 50 μg/ml streptomycin (Invitrogen Corporation) and incubated at 37°C in a humidified atmosphere of 5% CO_2. Once in exponential growth phase, the cells were harvested using trypsin/EDTA, washed, suspended in phosphate-buffered saline (PBS) and counted.

One million Panc 02 cells (in 50 μl PBS) [23] were injected subcutaneously in the right hind leg (thigh) of male HsdOla/MF1 mice. All animals were observed daily for general appearance, behavior, and tumor growth. Growth of the subcutaneous tumors was visually evaluated using a vernier calliper. Tumor surface area (cm^2) was calculated as [tumor width (horizontal diameter) × tumor length (vertical diameter)].

MRI

MRI was performed 24–28 days after tumor inoculation on a Siemens Magnetom Symphony 1.5-Tesla scanner (Siemens AG, Erlangen, Germany) with a wrist coil (four-channel high-resolution coil, 10 cm diameter, Siemens Invivo 1.5-T, Siemens AG, Erlangen, Germany). Animals were sedated with ketamine/xylazine during MRI procedures. First, a localizer was performed (slice thickness 10 mm, matrix size 128 × 256 mm, field of view 200 mm, echo time 5 ms, repetition time 15 ms, flip angle 40°). Imaging comprised a single axial slice that was positioned through both upper limbs and the center of the tumor as localizer. Before contrast injection, $T1$ zero time maps were constructed from 2 spin echo sequences with different repetition times (1,000 and 318 ms, respectively). This was followed by a $T2$-weighted sequence before contrast administration for tumor localization and visualization of extratumoral tissues. Details of the sequence were as follows: temporal resolution 24 s, field of view 113 mm, matrix size 192 × 256, slice thickness 3 mm, echo time 67 ms, repetition time 1,210 ms, and flip angle 150°. Dynamic imaging was performed using an IR-Turbo-FLASH sequence centered through both upper limbs and the center of the tumor. Details of the pulse sequence were as follows: repetition time 1,100 ms, field of view 100 mm, matrix size 128 × 256 mm, slice thickness 5 mm, echo time 4.08 ms, inversion time 560 ms, and flip angle 12°.

A bolus of contrast was manually injected into the tail vein after the 4th scan. In total, 500 images were obtained for a total scan time of 550 s.

MRI contrast agents

Each animal was randomly assigned to one of the three DCE-MRI contrast agents (CA) involved in this study: Gd-DOTA, P846, and P792. All contrast agents were obtained from Guerbet Research (Roissy, France).

Table 1 Properties of the MR contrast agents used

	Gd-DOTA[a]	P846[b]	P792[c]
Molecular weight (kDa)	0.5	3.5	6.5
T1 Relaxivity ($mM^{-1}s^{-1}$)*	3.4	32	27
Dose (μmol Gd/kg)	100	25	40
Tumor area (cm^2)	1.35 ± 0.59	1.95 ± 0.75	1.64 ± 0.97
p-value	0.588[ab]	0.387[bc]	0.206[ac]

The letters a, b and c were used to facilitate comparison of tumor area groups in the last line of the table (p-values)
kDa, kiloDalton
* At 1.5 Tesla and 37°C. Tumor areas were expressed as mean ± standard deviation

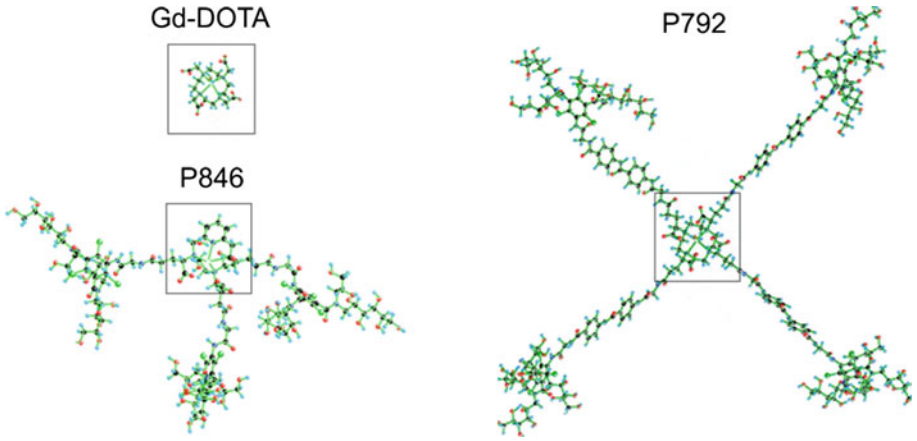

Fig. 1 Molecular structure of the contrast agents used

The physicochemical properties and dosages used are summarized in Table 1. The used dosages were determined empirically by the manufacturer, taking into account differences in $T1$ relaxivity of the compounds [24,25].

Gd-DOTA (gadoterate meglumine) is a paramagnetic ionic extracellular CA used in daily practice. P846 is a low diffusion agent, consisting of a macrocyclic gadolinium chelate (Fig. 1). The product is renally excreted, but extravasation through normal endothelium is slow due to its physical size. P792 (gadomelitol) is a macromolecular Gd-DOTA derivate, originally developed as a blood pool agent with rapid clearance and mainly free renal elimination. The molecular structure of the agents is illustrated in Fig. 1.

Analysis of MRI images

Postprocessing was performed using the research mode of a commercially available software tool (MIStar^{TM}, Apollo Medical Imaging, Melbourne, Australia). Both a qualitative description of the tissue enhancement curve and a two-compartment pharmacokinetic approach according to Tofts and Kermode were implemented [26]. In each tumor, regions of interest (ROIs) were manually tracked to cover the entire tumor circumference (ROI 1) and normal muscle tissue (ROI 2). In each ROI, the area under the enhancement curve (AUC, until 550 s after contrast arrival) was calculated.

The IR-TurboFLASH signal intensity varies with the longitudinal and transverse relaxation rates $R_1(= 1/T1)$ and $R_2*(= 1/T2*)$ as follows:

$$S(R_1, R_2^*) = M_0 \sin(\alpha) \times \frac{1 - 2\exp(-R_1\mathrm{TI}) + \exp(-R_1\mathrm{TR})}{1 + \cos(\alpha)\exp(-R_1\mathrm{TR})} \exp(-T_\mathrm{E} R_2^*)$$

[26,27]. M_0 is a scaling factor, comprising equilibrium magnetization and proton density. TI is the inversion time, TR is the repetition time, and α is the flip angle. For DCE-MRI, the relation between relaxation rate and contrast agent concentration C is generally assumed to be linear:

$$R_1 = R_{10} + r_1 C$$

where R_1 is the relaxivity coefficient of the contrast agent and R_{10} is the native relaxation rate $(= 1/T_{10})$, available from the precontrast $T1$-mapping experiment. Pharmacokinetic modeling was based on the modified Tofts two-compartment model, which accounts for a vascular input component and defines a vascular space and an extravascular, extracellular space (EES). The kinetic behavior of the injected CA is modeled as a diffusive transport process based on Fick's law.

The tissue CA concentration, C_t, is given by:

$$C_\mathrm{t} = v_\mathrm{p} C_\mathrm{p}(t) + K^\mathrm{trans} \int_0^t C_\mathrm{p}(t') e^{\frac{-K^\mathrm{trans}}{v_\mathrm{e}}(t-t')} \mathrm{d}t'$$

where K^trans $(\times$ 1,000/min) denotes the transfer constant, V_p the fractional vascular space ($\times$ 1,000, dimensionless), V_e the fraction of the interstitial space ($\times$ 1,000, dimensionless) entered by the CA, and C_p the plasma concentration (in mM). In each tumor, the pixel with the most representative arterial input function was manually selected from the femoral artery of the tumor-bearing leg or the opposite leg to provide $C_\mathrm{p}(t)$. Tissue concentrations were calculated based on the $T1$ maps. These data, together with the selected arterial input function, were used as the input for a curve fitting routine resulting in parametric maps of K^trans and V_e. In the Gd-DOTA group, 8/10 animals had exploitable MRI data, with 5 and 7 animals for the P846 and P792 groups, respectively. Quantitative values for all pixels in the different regions of interest described above were exported to a spread sheet for further analysis. Tumor-to-muscle ratios are presented in Fig. 4.

Statistics

Data are expressed as mean $\pm$ standard deviation, unless stated otherwise. Differences between two groups of continuous data were assessed by the independent-sample Student's

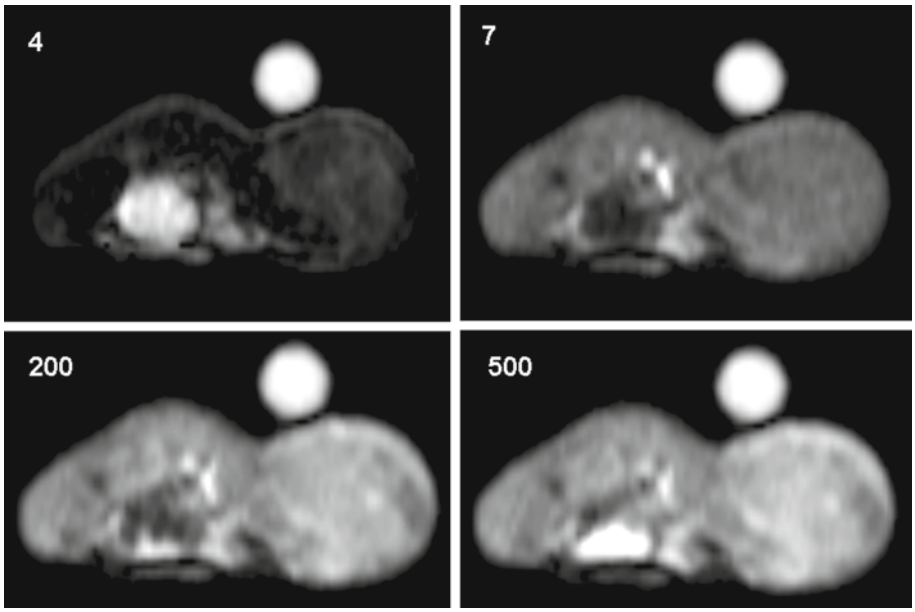

Fig. 2 Typical enhancement pattern after 4, 7, 200, and 500 images following the injection of P792 after image 4. The tumor is located in the *right lower limb* (mouse in prone position). A vitamin A pearl is used to aid in positioning the tumor

t-test or the nonparametric Mann–Whitney *U*-test. The mean tumor surface areas were compared for all contrast groups using one-way ANOVA. Statistical significance was defined as $p < 0.05$. All statistics were calculated using SPSS for Windows (version 15.0, IBM Corporation, New York, USA).

Results

Molecular structures of the used contrast agents are depicted in Fig. 1. Tumor areas for the different contrast agent groups are shown in Table 1. No significant differences in tumor area were found between the different contrast groups.

Different temporal enhancement patterns were observed according to the CA used. When DCE-MRI was performed with P792, the largest agent, slow enhancement of the tumor was observed with a peak after approximately 5 min (Figs. 2, 3). Normal muscle showed very little enhancement when using P792. As expected for an agent that was originally developed as a blood pool contrast agent, the vascular input signal intensity did not return to baseline after 550 s.

AUC values were higher in tumor tissue than the levels observed in muscle tissue, although no significant difference was found when P846 was used as a contrast agent (Table 2). Tumor/muscle tissue enhancement was lowest when using P846 (Fig. 4).

Values of K^{trans} decreased with the increase in molecular weight of contrast agents, a result that was confirmed by other authors [28]. Use of the lowest molecular weight agent Gd-DOTA resulted in the highest K^{trans} values, whereas use of P792, the highest molecular weight product, resulted in a low volume transfer coefficient. Following this trend, values of K^{trans} for P846 were intermediate between the values obtained with P792 and Gd-DOTA. Mann–Whitney *U*-test was used to compare parameters across contrast agents (*p*-values of 0.000, 0.06, and 0.007 were obtained when

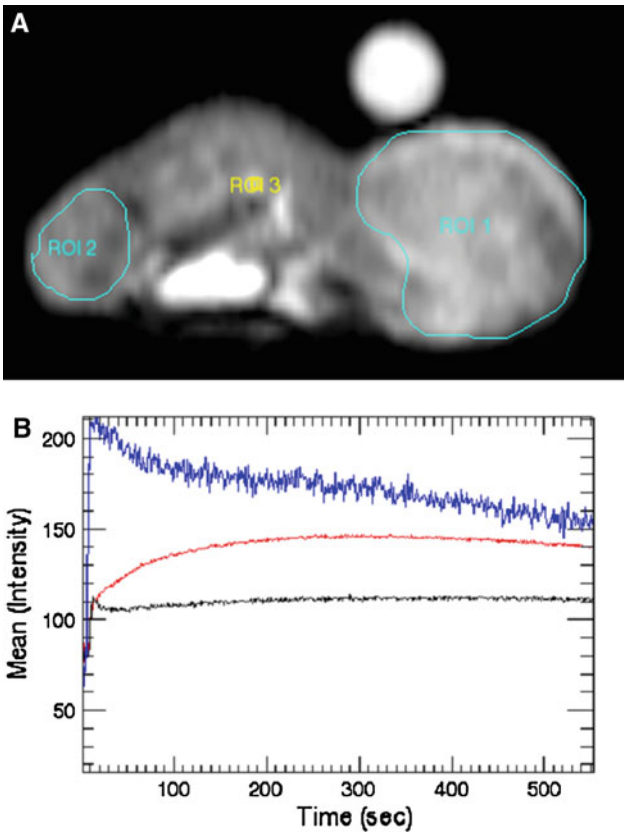

Fig. 3 **a** Regions of interest encompassing the tumor (*1*), muscle (*2*), and feeding artery (*3*). **b** Typical enhancement over time in muscle (*black curve*), tumor (*red curve*), and arterial input (*blue curve*)

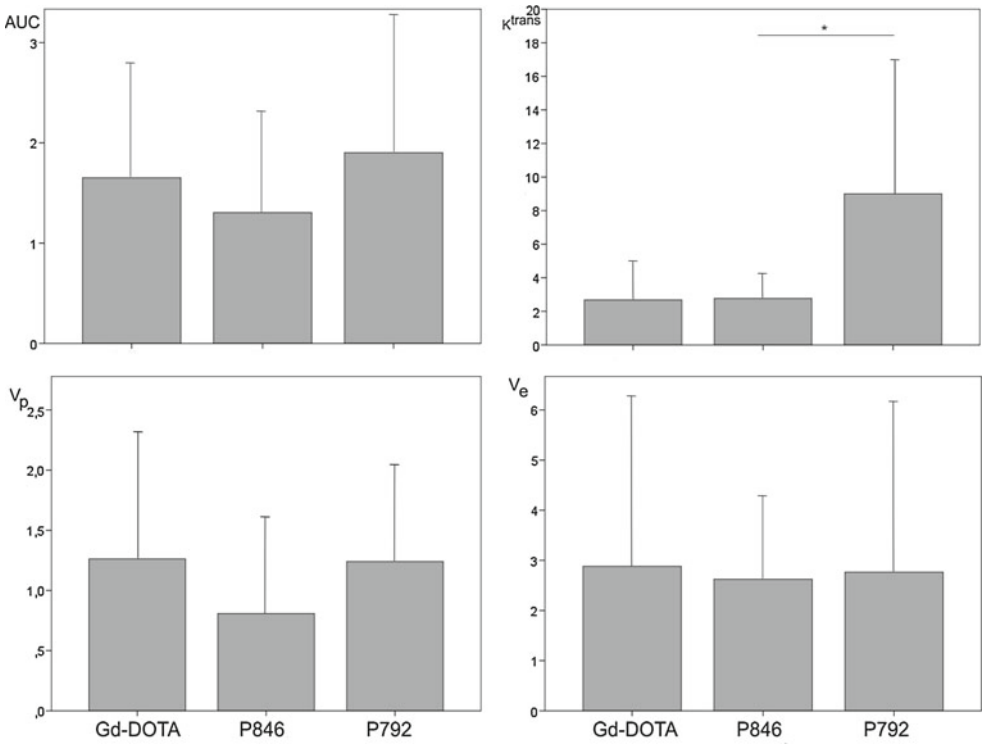

Fig. 4 Comparison of DCE-MRI vascular parameters for different contrast agents; tumor-to-muscle ratios are shown (mean ± standard deviation). AUC = area under enhancement curve; K^{trans} = volume transfer constant; V_e = interstitial leakage space fraction; V_p = fractional plasma volume. Significant differences between groups are indicated with *($p < 0.05$)

Table 2 DCE-MRI vascular parameters for the different contrast agents

	AUC	K^{trans} (× 1,000/ min)	V_e (fraction × 1,000)	V_p (fraction ×1,000)
Gd-DOTA				
Tumor	682 ± 295	174 ± 129	487 ± 402	178 ± 113
Muscle	413 ± 221	64.9 ± 57.1	169 ± 113	141 ± 103
p-value	0.001	0.003	0.007	0.475
P846				
Tumor	411 ± 248	74.4 ± 37.3	102 ± 37.0	27.3 ± 17.4
Muscle	315 ± 217	26.9 ± 19.7	38.9 ± 21.1	33.8 ± 20.3
p-value	0.162	<0.001	<0.001	0.234
P792				
Tumor	557 ± 332	16.3 ± 12.5	52.0 ± 24.0	22.2 ± 8.25
Muscle	293 ± 194	1.81 ± 1.47	18.8 ± 6.90	17.9 ± 9.40
p-value	0.003	<0.001	<0.001	0.118

Results (mean ± standard deviation are expressed as K^{trans}*1,000/ min; V_e*1,000 and V_p*1,000)

comparing Gd-DOTA/P792, Gd-DOTA/P846, and P846/P792, respectively). When comparing tumor tissue with reference tissue, as illustrated in Fig. 4 and Table 2, values for K^{trans} were significantly lower in control tissue, for all contrast agents studied.

The obtained results for the fraction of the interstitial leakage space V_e follow the same trend as the values for K^{trans}: lowest values were demonstrated after the use of P792, the highest values were seen using Gd-DOTA. Again, the use of P846 resulted in intermediate V_e values (Mann–Whitney *U*-test *p*-values were 0.000, 0.000 and 0.086 for Gd-DOTA/P792, Gd-DOTA/P846, and P846/P792, respectively). Also, a significant reduction in V_e was noticed in control tissue (Table 2). This reduction was comparable for all contrast agents. As an exception, no significant difference between tumor and muscle tissue could be

observed for V_p. Highest V_p values were obtained with Gd-DOTA.

Figure 4 illustrates the discriminatory properties of the contrast agents used. Calculation of the AUC did not improve differentiation between tumor tissue and normal muscle. However, the tumor/muscle ratio of the transfer constant was significantly higher for P792 than for P846 or Gd-DOTA ($p < 0.001$, Mann–Whitney U-test). No significant differences were observed in the estimated plasma or interstitial volume ratio.

Discussion

The main advantage of dynamic contrast-enhanced magnetic resonance imaging (DCE-MRI) is its noninvasive nature, allowing the calculation of several vascular parameters. These parameters (K^{trans}, V_e, and V_p) can be used to characterize individual tumor types; for example, to distinguish malignant from benign tissue and to monitor tumor response to antitumoral therapy noninvasively.

Currently, only contrast agents with low molecular weight are used in clinical settings. These products show rapid extravasation through both tumor and normal blood vessels. Contrast agents with high molecular weight show only limited extravasation through normal blood vessels. The higher permeability of most tumor vasculature allows these contrast agents to penetrate the tumor and thus provide better tumor detection/identification with DCE-MRI.

In this study, the influence of contrast agents with intermediate molecular weight on the selective DCE-MRI contrast enhancement in Panc02 pancreas tumors was investigated, using normal muscle tissue as control. The results were compared with the clinically used contrast agent Gd-DOTA. Our results demonstrate that the values of vascular parameters K^{trans} and V_e are dependent on the size and molecular weight of the used contrast agent.

The significantly lower values of K^{trans} in muscle tissue compared with tumor tissue indicate a larger vascular permeability of the contrast agent in tumor tissue. It is generally accepted that low molecular weight gadolinium-based contrast agents often overestimate tumor blood volume and vascular permeability because of their rapid extravasation from blood to the extracellular space in tumor tissue [29]. On the other hand, macromolecular contrast agents have been shown to provide more accurate tumor characterization and are better able to differentiate tumor vascular permeability [30]. Our results indicate that this can also be applied for contrast agents with intermediate molecular weight, such as P792 and—to a lesser extent—P846. Intermediate molecular weight contrast agents have restricted diffusion through the endothelium, but can pass freely through the glomerular membrane [10]. The uptake of P792 and P846 is more strongly influenced by capillary permeability, while that of the low molecular weight Gd-DOTA is more heavily influenced by perfusion [31]. The potential of higher molecular weight contrast agents to discriminate tumor from muscle tissue is also reflected in the lower obtained p-values for these contrast agents, as illustrated in Table 2.

The relative increase in tumor K^{trans} (compared with muscle tissue) was also calculated: an increase with a factor ~ 2.7 was obtained for Gd-DOTA and P846, whereas a 9-fold increase was observed for P792. However, absolute K^{trans} values were lowest using P792.

For the kinetic analysis of the MRI images, one ROI was drawn around the entire tumor perimeter and another ROI was drawn on the contralateral thigh muscle tissue. Differences in tumor vascular properties between the core and the rim of the tumor were found by other authors [9]. However, in this study, no significant differences in DCE-MRI parameters were found between tumor core and rim (data not shown).

When interpreting the obtained values for the vascular kinetic parameters, the balance between blood flow and capillary permeability in the tissue of interest has to be taken into account [32]. K^{trans} is a function of flow (perfusion) and permeability [33]. In high-permeability situations, K^{trans} represents the blood plasma flow. In cases of low permeability, K^{trans} is influenced more by the permeability surface area, and concentration of contrast agent mainly depends on the ability of the contrast agent to penetrate the target tissue. This ability is strongly influenced by molecular weight (and molecular volume) of the used contrast agent. The assumption that K^{trans} represents the tumor microvessel permeability surface area product when using higher molecular weight contrast agents, and that flow is represented when low molecular weight contrast agents are used, seems supported in this study: use of the lowest MW agent Gd-DOTA resulted in the highest absolute K^{trans} values. This result was also confirmed by other authors [9].

In contrast to the data obtained for K^{trans} and V_e, no significant differences between tumor and muscle tissue were observed for V_p. Other authors have also reported this discrepancy for V_p or comparable parameters [28]. K^{trans} appears to be a more sensitive parameter than V_p for the evaluation of DCE-MRI kinetics. However, small sample size ($n = 5$ for P846) and large experimental errors—combined with the inherent relatively low signal-to-noise ratio of MR imaging—may contribute to this lack of statistical significance.

Conclusion

The influence of using gadolinium-based contrast agents with different molecular weights on the dynamic contrast-enhanced MRI kinetic parameters K^{trans}, V_e, and V_p was

investigated in a Panc02 pancreatic tumor model in mice. Two contrast agents with intermediate molecular weight (P846, 3.5 kDa and P792, 6.47 kDa) and one with low molecular weight (Gd-DOTA, 0.5 kDa) were used in this study.

We demonstrated that values for K^{trans} and V_e are highly dependent on the molecular weight of the contrast agent used. Our results indicate that, compared with low MW products, intermediate MW contrast agents (such as P792 and P846) are better able to differentiate tumor from muscle tissue. Intermediate MW contrast agents can provide a tool for early therapy response imaging and quantification.

Acknowledgments This study could not have been conducted without the invaluable contribution of Philippe Robert, Experimental Imaging Division Manager of the Research Department of Guerbet Group, Paris, France, and special thanks for providing the contrast agents investigated in this study.

References

1. Jemal A, Siegel R, Xu J, Ward E (2010) Cancer statistics, 2010. CA Cancer J Clin 60:277–300
2. Folkman J (1992) The role of angiogenesis in tumor growth. Semin Cancer Biol 3:65–71
3. McDonald DM, Choyke PL (2003) Imaging of angiogenesis: from microscope to clinic. Nat Med 9:713–725
4. Weidner N, Folkman J, Pozza F, Bevilacqua P, Allred EN, Moore DH, Meli S, Gasparini G (1992) Tumor angiogenesis: a new significant and independent prognostic indicator in early-stage breast carcinoma. J Natl Cancer Inst 84:1875–1887
5. Daldrup H, Shames DM, Wendland M, Okuhata Y, Link TM, Rosenau W, Lu Y, Brasch RC (1998) Correlation of dynamic contrast-enhanced MR imaging with histologic tumor grade: comparison of macromolecular and small-molecular contrast media. AJR Am J Roentgenol 171:941–949
6. Schwickert HC, Stiskal M, Roberts TP, van Dijke CF, Mann J, Muhler A, Shames DM, Demsar F, Disston A, Brasch RC (1996) Contrast-enhanced MR imaging assessment of tumor capillary permeability: effect of irradiation on delivery of chemotherapy. Radiology 198:893–898
7. Padhani AR (2002) Functional MRI for anticancer therapy assessment. Eur J Cancer 38:2116–2127
8. Dvorak HF, Nagy JA, Dvorak JT, Dvorak AM (1988) Identification and characterization of the blood vessels of solid tumors that are leaky to circulating macromolecules. Am J Pathol 133:95–109
9. de Lussanet QG, Langereis S, Beets-Tan RG, van Genderen MH, Griffioen AW, van Engelshoven JM, Backes WH (2005) Dynamic contrast-enhanced MR imaging kinetic parameters and molecular weight of dendritic contrast agents in tumor angiogenesis in mice. Radiology 235:65–72
10. Fan X, Medved M, Foxley S, River JN, Zamora M, Karczmar GS, Corot C, Robert P, Bourrinet P (2006) Multi-slice DCE-MRI data using P760 distinguishes between metastatic and non-metastatic rodent prostate tumors. Magn Reson Mater Phy 19:15–21
11. Turetschek K, Floyd E, Helbich T, Roberts TP, Shames DM, Wendland MF, Carter WO, Brasch RC (2001) MRI assessment of microvascular characteristics in experimental breast tumors using a new blood pool contrast agent (MS-325) with correlations to histopathology. J Magn Reson Imaging 14:237–242
12. Brurberg KG, Benjaminsen IC, Dorum LM, Rofstad EK (2007) Fluctuations in tumor blood perfusion assessed by dynamic contrast-enhanced MRI. Magn Reson Med 58:473–481
13. Ceelen W, Boterberg T, Smeets P, Van Damme N, Demetter P, Zwaenepoel O, Cesteleyn L, Houtmeyers P, Peeters M, Pattyn P (2007) Recombinant human erythropoietin alpha modulates the effects of radiotherapy on colorectal cancer microvessels. Br J Cancer 96:692–700
14. Ceelen W, Smeets P, Backes W, Van Damme N, Boterberg T, Demetter P, Bouckenooghe I, De Visschere M, Peeters M, Pattyn P (2006) Noninvasive monitoring of radiotherapy-induced microvascular changes using dynamic contrast enhanced magnetic resonance imaging (DCE-MRI) in a colorectal tumor model. Int J Radiat Oncol 64:1188–1196
15. Brasch RC, Li KCP, Husband JE, Keogan MT, Neeman M, Padhani AR, Shames D, Turetschek K (2000) In vivo monitoring of tumor angiogenesis with MR imaging. Acad Radiol 7:812–823
16. Taylor JS, Tofts PS, Port R, Evelhoch JL, Knopp M, Reddick WE, Runge VM, Mayr N (1999) MR imaging of tumor microcirculation: promise for the new millennium. J Magn Reson Imaging 10:903–907
17. Yuh WT (1999) An exciting and challenging role for the advanced contrast MR imaging. J Magn Reson Imaging 10:221–222
18. Chang EY, Li X, Jerosch-Herold M, Priest RA, Enestvedt CK, Xu J, Springer CS Jr, Jobe BA (2008) The evaluation of esophageal adenocarcinoma using dynamic contrast-enhanced magnetic resonance imaging. J Gastrointest Surg 12:166–175
19. de Lussanet QG, Backes WH, Griffioen AW, Padhani AR, Baeten CI, van Baardwijk A, Lambin P, Beets GL, van Engelshoven JM, Beets-Tan RG (2005) Dynamic contrast-enhanced magnetic resonance imaging of radiation therapy-induced microcirculation changes in rectal cancer. Int J Radiat Oncol Biol Phys 63:1309–1315
20. Ocak I, Bernardo M, Metzger G, Barrett T, Pinto P, Albert PS, Choyke PL (2007) Dynamic contrast-enhanced MRI of prostate cancer at 3 T: a study of pharmacokinetic parameters. AJR Am J Roentgenol 189:849
21. Yankeelov TE, Gore JC (2009) Dynamic contrast enhanced magnetic resonance imaging in oncology: theory, data acquisition, analysis, and examples. Curr Med Imaging Rev 3:91–107
22. Yankeelov TE, Lepage M, Chakravarthy A, Broome EE, Niermann KJ, Kelley MC, Meszoely I, Mayer IA, Herman CR, McManus K, Price RR, Gore JC (2007) Integration of quantitative DCE-MRI and ADC mapping to monitor treatment response in human breast cancer: initial results. Magn Reson Imaging 25:1–13
23. Casneuf VF, Demetter P, Boterberg T, Delrue L, Peeters M, Van Damme N (2009) Antiangiogenic versus cytotoxic therapeutic approaches in a mouse model of pancreatic cancer: an experimental study with a multitarget tyrosine kinase inhibitor (sunitinib), gemcitabine and radiotherapy. Oncol Rep 22:105–113
24. Port M, Corot C, Rousseaux O, Raynal I, Devoldere L, Idee JM, Dencausse A, Le Greneur S, Simonot C, Meyer D (2001) P792: a rapid clearance blood pool agent for magnetic resonance imaging: preliminary results. Magn Reson Mater Phy 12:121–127
25. Jacquier A, Bucknor M, Do L, Robert P, Corot C, Higgins CB, Saeed M (2008) P846, a new gadolinium based low diffusion magnetic resonance contrast agent, in characterizing occlusive infarcts, reperfused ischemic myocardium and reperfused infarcts in rats. Magn Reson Mater Phy 21:207–218
26. Tofts PS (1997) Modeling tracer kinetics in dynamic Gd-DTPA MR imaging. JMRI-J Magn Reson Imaging 7:91–101
27. De Naeyer D, De Deene Y, Ceelen WP, Segers P, Verdonck P (2011) Precision analysis of kinetic modelling estimates in dynamic contrast enhanced MRI. Magn Reson Mater Phy 24:51–66
28. Wu X, Jeong EK, Emerson L, Hoffman J, Parker DL, Lu ZR (2010) Noninvasive evaluation of antiangiogenic effect in a mouse tumor model by DCE-MRI with Gd-DTPA cystamine copolymers. Mol Pharm 7:41–48

29. Brasch RC (1992) New directions in the development of MR imaging contrast media. Radiology 183:1–11
30. van Dijke CF, Brasch RC, Roberts TP, Weidner N, Mathur A, Shames DM, Mann JS, Demsar F, Lang P, Schwickert HC (1996) Mammary carcinoma model: correlation of macromolecular contrast-enhanced MR imaging characterizations of tumor microvasculature and histologic capillary density. Radiology 198:813–818
31. Fan X, Medved M, River JN, Zamora M, Corot C, Robert P, Bourrinet P, Lipton M, Culp RM, Karczmar GS (2004) New model for analysis of dynamic contrast-enhanced MRI data distinguishes metastatic from nonmetastatic transplanted rodent prostate tumors. Magn Reson Med 51:487–494
32. Tofts PS, Brix G, Buckley DL, Evelhoch JL, Henderson E, Knopp MV, Larsson HB, Lee TY, Mayr NA, Parker GJ, Port RE, Taylor J, Weisskoff RM (1999) Estimating kinetic parameters from dynamic contrast-enhanced T(1)-weighted MRI of a diffusable tracer: standardized quantities and symbols. J Magn Reson Imaging 10:223–232
33. Choyke PL, Dwyer AJ, Knopp MV (2003) Functional tumor imaging with dynamic contrast-enhanced magnetic resonance imaging. J Magn Reson Imaging 17:509–520